The Plant Cell, Vol. 19: 1473–1487, May 2007, www.plantcell.org © 2007 American Society of Plant Biologists

CYP703 Is an Ancient Cytochrome P450 in Land Plants Catalyzing in-Chain Hydroxylation of Lauric Acid to Provide Building Blocks for Sporopollenin Synthesis in Pollen [W]

Marc Morant,[a] Kirsten Jørgensen,[a] Hubert Schaller,[b] Franck Pinot,[b] Birger Lindberg Møller,[a] Danièle Werck-Reichhart,[b] and Søren Bak[a,1]

[a] Plant Biochemistry Laboratory, Department of Plant Biology and Center for Molecular Plant Physiology, Faculty of Life Sciences, University of Copenhagen, DK-1871 Frederiksberg C, Copenhagen, Denmark

[b] Departments of Plant Metabolic Responses and Plant Isoprenoids, Botanic Institute, Louis Pasteur University, 67083 Strasbourg Cedex, France

CYP703 is a cytochrome P450 family specific to land plants. Typically, each plant species contains a single CYP703. *Arabidopsis thaliana CYP703A2* is expressed in the anthers of developing flowers. Expression is initiated at the tetrad stage and restricted to microspores and to the tapetum cell layer. *Arabidopsis CYP703A2* knockout lines showed impaired pollen development and a partial male-sterile phenotype. Scanning electron and transmission electron microscopy of pollen from the knockout plants showed impaired pollen wall development with absence of exine. The fluorescent layer around the pollen grains ascribed to the presence of phenylpropanoid units in sporopollenin was absent in the *CYP703A2* knockout lines. Heterologous expression of CYP703A2 in yeast cells demonstrated that CYP703 catalyzes the conversion of medium-chain saturated fatty acids to the corresponding monohydroxylated fatty acids, with a preferential hydroxylation of lauric acid at the C-7 position. Incubation of recombinant CYP703 with methanol extracts from developing flowers confirmed that lauric acid and in-chain hydroxy lauric acids are the in planta substrate and product, respectively. These data demonstrate that in-chain hydroxy lauric acids are essential building blocks in sporopollenin synthesis and enable the formation of ester and ether linkages with phenylpropanoid units. This study identifies CYP703 as a P450 family specifically involved in pollen development.

INTRODUCTION

Plants began to colonize land 450 to 600 million years ago. The transition from water to land required adaptation to more extreme light, temperature, and water conditions. An essential prerequisite for this step was the ability to protect the ungerminated gametophyte. A key element in this strategy was the development of sporopollenin, a biopolymer in spores from mosses and in pollen. Sporopollenin constitutes the main constituent of exine, the outer layer of spores and pollen. Exine not only affords a protective barrier against pathogen attack, dehydration, and UV irradiation but also facilitates pollen recognition and adhesion to the stigma and thus has a role in protection as well as pollination (Edlund et al., 2004). Although sporopollenin is an essential contributor to important exine characteristics, the chemical composition of this polymer remains elusive, as it is difficult to chemically degrade into defined components and to isolate in large amounts. Studies on the chemical similarities between the wall of spores and pollen and on the composition of sporopollenin were first reported in 1937 (Zetzsche et al., 1937). Recently, based on acidic methanolysis of exine from cattail (*Typha angustifolia*), sporopollenin was proposed to be composed of a limited number of different monomers (Bubert et al., 2002). Polyhydroxylated unbranched aliphatic units as well as phenolic constituents were identified as the main monomeric units in different plant taxa (Wehling et al., 1989; Ahlers et al., 1999, 2000; Bohne et al., 2003). High-resolution solid state ^{13}C NMR spectroscopy identified oxygen atoms present in ether, aliphatic and phenolic hydroxy, carboxy, and ester groups (Guilford et al., 1988; Ahlers et al., 2003). Covalent coupling of the monomeric units of sporopollenin by ether linkages has been proposed to provide the characteristic high resistance to chemical degradation (Ahlers et al., 2000). Studies of *Arabidopsis thaliana* male-sterile mutants with abnormal exine formation have shown that tapetal cells as well as the pollen grain contribute to exine biosynthesis (Bedinger, 1992). Analysis of the male-sterile mutants *male sterile2* (*ms2*) (Aarts et al., 1997), *defective in exine patterning1* (*dex1*) (Paxson-Sowders et al., 2001), *no exine formation1* (*nef1*) (Ariizumi et al., 2004), and *faceless pollen1* (*flp1*) (Ariizumi et al., 2003) indicate the incorporation of fatty acids and the transport of components from the sporophytic surroundings as integral steps in sporopollenin deposition.

Cytochromes P450 (P450s) are hemethiolate monooxygenases involved in a vast array of biosynthetic pathways in secondary and primary metabolism (Werck-Reichhart et al., 2002; Morant et al., 2003). P450s involved in the synthesis of pivotal

[1] To whom correspondence should be addressed. E-mail bak@life.ku.dk; fax 45-35-28-33-33.
The author responsible for distribution of materials integral to the findings presented in this article in accordance with the policy described in the Instructions for Authors (www.plantcell.org) is: Søren Bak (bak@life.ku.dk).

[W] Online version contains Web-only data.

www.plantcell.org/cgi/doi/10.1105/tpc.106.045948

backbone structures characteristic of different classes of primary and secondary metabolites are highly conserved throughout the plant kingdom (e.g., CYP73, the cinnamic acid 4-hydroxylase, catalyzing the initial step in phenylpropanoid synthesis; and CYP51, catalyzing the essential 14α-demethylation step in sterol biosynthesis) (Nelson et al., 2004). Based on phylogenetic studies, plant P450s can be divided into 10 separate clans that cover the current 61 families (Nelson et al., 2004; Galbraith and Bak, 2005; http://www.p450.kvl.dk/p450.shtml). The demand for the recruitment of novel catalytic abilities and for enhanced substrate profiles is reflected by a large number of duplication events. Accordingly, most P450 families in higher plants are proliferated and contain multiple paralogs. As an example of this, 273 DNA sequences encoding P450s have been identified in the fully sequenced *Arabidopsis* genome (http://www.p450.kvl.dk/p450.shtml). Based on the biochemistry catalyzed by known P450s from the 10 different clans, plant P450s can been divided into three major groups. The first diverse and ancient group includes P450s with a function that preceded the colonization of land by plants. This group is extant in *Chlamydomonas reinhardtii* and contains clans 51 and 710, involved in sterol biosynthesis; clan 97, involved in the biosynthesis of carotenoids; and clan 711, the function of which is unknown. The second group includes P450s that evolved as a consequence of the development of multicellular terrestrial life forms, as represented by clan 85, involved in the biosynthesis of hormones for signaling and development (e.g., brassinosteroids and gibberellins); clan 74, involved in jasmonic acid biosynthesis; and fatty acid monohydroxylases in clan 86, required for cutin synthesis. The third group comprises the highly proliferated clan 71. This clan includes P450s involved in the biosynthesis of the majority of plant natural products involved in adaptation to abiotic and biotic stress (e.g., P450s involved in lignin and flavonoid synthesis).

While most P450 families have proliferated through time, it is striking that four families (CYP703, CYP715, CYP722, and CYP724) are represented by single members in *Arabidopsis* as well as in *Oryza sativa* (Nelson et al., 2004). The fact that these four families exist as discrete and highly conserved single family members across taxa strongly indicates that they encode an essential and conserved biological function. Of these four single family members, a function has been assigned to CYP724. CYP724 is involved in the early C-22 hydroxylation step in brassinolide biosynthesis common to all land plants (Ohnishi et al., 2006). The CYP703 family has been studied in *Petunia hybrida*, in which the gene was shown to be expressed in the early stage of flower bud development. Although recombinant petunia CYP703A1 was shown to convert lauric acid into unknown products, the biological function of the CYP703 family has remained elusive (Imaishi et al., 1999).

Here, we show that the CYP703 family is present in all land plants examined. We demonstrate that *Arabidopsis CYP703A2* is expressed during pollen development. Knockout of *CYP703A2* impairs pollen development, as the exine is not developed, and results in a male-semisterile phenotype. Heterologous expression of CYP703A2 identified capric (C10), lauric (C12), and myristic (C14) acids as saturated fatty acid substrates and identified the products formed as the corresponding in-chain monohydroxylated fatty acids preferentially hydroxylated at carbon atom 7. Methanol extracts from developing flowers identified lauric acid and in-chain hydroxy lauric acid as the in planta substrate and product, respectively. This indicates that in-chain hydroxylated fatty acids are key components in sporopollenin synthesis during exine formation and identifies CYP703 as a P450 family specifically involved in pollen development.

RESULTS

The CYP703 Family Evolved with Land Colonization and Is Conserved among Land Plants

EST databases constitute a powerful resource to survey the species and tissues in which a gene is expressed. EST databases were mined with *Arabidopsis* CYP703A2 (At1g01280) as the query, and 43 putative CYP703 ESTs were identified from 17 different species (Table 1), mainly belonging to angiosperms and gymnosperms. The overrepresentation in angiosperms corresponds to the larger number of angiosperm ESTs present in public plant databases. Based on the available data, *CYP703* appears to be a single-family gene in seed plants. The recent availability of the genome of the moss *Physcomitrella patens* (http://moss.nibb.ac.jp/cgi-bin/blast-assemble) allowed for a search for CYP703 orthologs in nonvascular plants. Three putative CYP703 orthologs were identified in the moss. Full-length coding sequences were identified by contig assembly, and homology with the CYP703 family was confirmed by phylogenetic analyses (Figure 1). According to the general nomenclature rules, P450s are assigned to the same family when the sequence identity at the amino acid level is >50%. The three moss sequences show <50% amino acid sequence identity to CYP703A1. A phylogenetic analysis clearly documented that the three *P. patens* orthologs truly belong to the 703 clade. Accordingly, they have been assigned as CYP703B1, CYP703B2, and CYP703B3 (Figure 1). No ortholog could be identified in the genome of the green alga *C. reinhardtii* (http://www.chlamy.org). In conclusion, this survey shows that CYP703 is ubiquitously present in land plants but is absent in green algae.

CYP703A2 Expression Is Restricted to Developing Anthers

The EST analysis revealed that the ESTs identified by the data mining were all derived from libraries constructed from tissues including flower buds or flowers and that a majority of the ESTs were isolated from early stages of flower development or preanthesis (Table 1). Publicly available microarray databases such as Genevestigator (Zimmermann et al., 2004) provide an additional rich resource of information on the tissue expression of *Arabidopsis* genes. According to the Gene Atlas tool of Genevestigator, *CYP703A2* (*At1g01280*) is expressed in inflorescences but not in any other tissues.

The data mining indicated that *CYP703A2* is expressed in buds or flowers. To confirm this, RT-PCR using *CYP703A2*-specific primers was performed. RT-PCR showed that the *CYP703A2* transcript was readily detectable in closed flower buds but could not be detected in roots, leaves, stems, cauline leaves, green siliques, and open flowers (Figure 2). To determine the expression pattern of *CYP703A2* in planta at the tissue level, the first 1000 nucleotides upstream of the start codon of

Table 1. Occurrence of Putative *CYP703* Orthologs in EST and Genomic Databases

Taxonomic Group		Species	Tissues Used for Library	Accession Number
Green algae		*Chlamydomonas reinhardtii*	http://www.chlamy.org	No hits
Bryophytes		*Physcomitrella patens*	http://moss.nibb.ac.jp/cgi-bin/blast-assemble	Three contigs
Gymnosperms		*Ginkgo biloba*	*Gingko* microsporophyll	CB094452, CB094744
		Picea glauca	Male strobili developmental sequence	CK442130, CK442743, CK442745
		Pinus taeda	TriplEx pollen cone library	AW754540
		Amborella trichopoda	Early male flower bud	CV012183
Angiosperms	Monocots	*Aegilops speltoides*	Premeiotic anther	BQ841303
		Oryza sativa	Panicle (>10 cm)	C99519, AU094669, AU064265[a]
		Secale cereale	Anther before anthesis	BE495344, BF145314, CD453339, BE495003, BE494625, BE493881
		Triticum aestivum	Spike at meiosis	BJ211945, BJ218997, BJ219398
		Zea mays	Mixed stages of anther and pollen	AW506768
	Eudicots	*Arabidopsis thaliana*	Flower bud	AV535036, AV532990[b]
			Mixed tissues (including flower)	AA720028
		Lotus corniculatus	Flower bud	BP040316, BP034275[c]
		Populus trichocarpa	Male catkin	V050E11
		Antirrhinum majus	Whole plant (including flower)	AJ805079, AJ793628, AJ808979
		Ipomoea nil	Flower and flower bud	BJ567452, BJ574200, BJ558599, BJ554486
		Lactuca sativa	Mixed tissues	BQ994698, BU001758
		Solanum lycopersicum	3- to 8-mm flower bud	BI929405
			8 mm to preanthesis bud	BI931896, BI932066, BI932102
		Solanum tuberosum	Flower bud	CV506033, CV502932, CV504543

The different entries represent putative *Arabidopsis CYP703A2* orthologs that were identified in EST databases encompassing algae, bryophytes, gymnosperms, monocots, and eudicots. The strong bias for expression in flowers buds, male organs, and tissues before anthesis is apparent. Analyses at the genome level in *C. reinhardtii* and *P. patens* are shown at top.

[a] These ESTs correspond to *O. sativa CYP703A3*.

[b] These ESTs correspond to *Arabidopsis CYP703A2*.

[c] These ESTs correspond with 99.6% identity to *L. japonicus CYP703A7*.

CYP703A2, which spans the entire promoter, were fused to the β-glucuronidase (GUS) reporter gene. Sixteen independent $P_{CYP703A2}$*:GUS* lines were selected and analyzed in both the Wassilewskija and Columbia (Col-0) ecotypes. GUS staining was performed at different stages of plant development (stages 1, 3, and 6, according to Boyes et al. [2001]). All transgenic lines examined displayed the same distinct expression pattern and revealed that expression was restricted to anthers (Figure 3B). To more precisely determine the expression in anthers, plastic-embedded GUS-stained flower sections were analyzed. The tapetum cell layer and the microspores were identified as the cell types expressing *CYP703A2*. Expression was initiated at the tetrad stage (Figure 3G). During pollen maturation, the tapetum cells started to degenerate as their function was completed and *CYP703A2* expression vanished (Figures 3I and 3J).

CYP703A2 Knockout Mutants Have Reduced Fertility

Two T-DNA insertion lines in the *Arabidopsis* Col-0 ecotype, SALK_119582 (Alonso et al., 2003) and SLAT N56842 of *At1g01280*, were identified. The T-DNA insertions were mapped to exons 1 and 2, respectively (see Supplemental Figure 1 online). In both T-DNA insertion lines, the absence of *At1g01280* transcripts in developing flowers was verified by RT-PCR (data not shown). Both T-DNA insertion lines displayed the same visual phenotype, characterized by slightly longer inflorescences, an extended period of blooming, a reduced number of elongated siliques, and overall reduced seed set. Analysis of the primary inflorescences at maturity showed that 31 ± 7% ($n = 12$ plants) of the siliques failed to develop in the SLAT N56842 line and 30 ± 6% ($n = 10$ plants) failed to develop in the SALK_119582 line. By contrast, only 6 ± 3% ($n = 11$ plants) of siliques failed to develop in Col-0 wild-type plants. The impaired siliques were mainly located at the base of the inflorescences, while the more apical siliques appeared similar to wild-type siliques (Figure 4A). Two backcrosses using wild-type pollen confirmed that the phenotype observed is linked to the absence of CYP703A2. In both *CYP703A2* knockout lines, the anthers within the first flowers formed as the lower part of the inflorescence wilted and were supported by a very short filament (data not shown). In the middle part of the inflorescence, filaments were longer than within the flowers positioned below but still shorter than in the wild type, and pollen release was not observed (cf. Figures 4B and 4D). In apical flowers, the amount of pollen was reduced

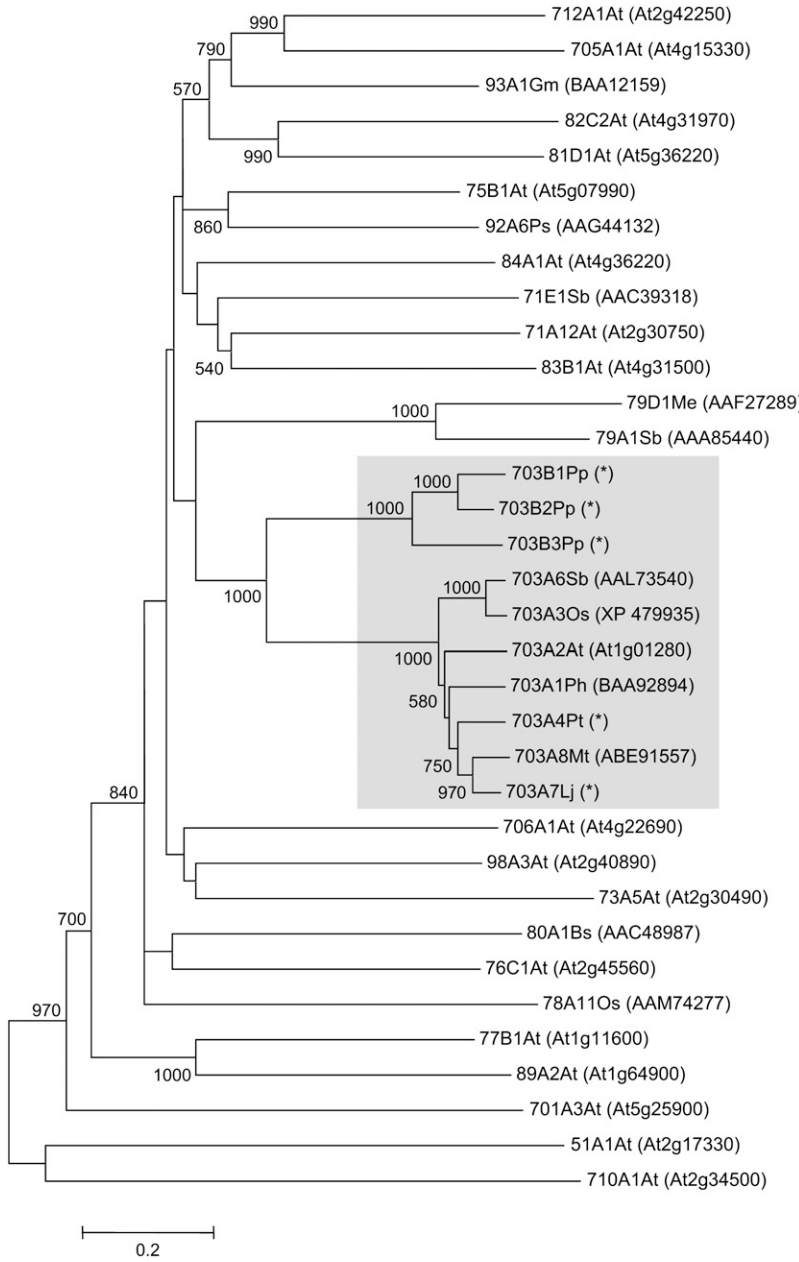

Figure 1. Phylogenetic Tree Displaying the Position of the CYP703 Family within the P450 71 Clan.

Bootstrap values are shown at the nodes. The CYP703 family is highlighted in gray. At, *Arabidopsis thaliana*; Bs, *Berberis stolonifera*; Gm, *Glycine max*; Lj, *Lotus japonicus*; Me, *Manihot esculenta*; Mt, *Medicago truncatula*; Ph, *Petunia hybrida*; Pp, *Physcomitrella patens*; Ps, *Pisum sativum*; Os, *Oryza sativa*; Sb, *Sorghum bicolor*. Sequences marked with asterisks were deduced from genomic data.

compared with the wild type, whereas filament length appeared similar to that of the wild type (cf. Figures 4A and 4C).

Scanning electron microscopy of pollen from middle and apical flowers revealed that the surface of the pollen from the mutant was smooth while the surface of wild-type pollen exhibited the characteristic ridged surface (Figures 4A to 4D). Cross-pollination of the *CYP703A2* insertion lines with wild-type pollen fully restored seed production, whereas wild-type plants crossed with pollen from the insertion lines resulted in a very poor seed production. This confirmed that the phenotype was associated with pollen, that pollen production was impeded, and that at least some of the pollen released was able to germinate. In agreement with this, pollen from the insertional lines germinated in vitro under high humidity (data not shown). The reduced seed production in the two *CYP703A2* knockout lines most likely reflected the combination of a reduced amount of mature pollen,

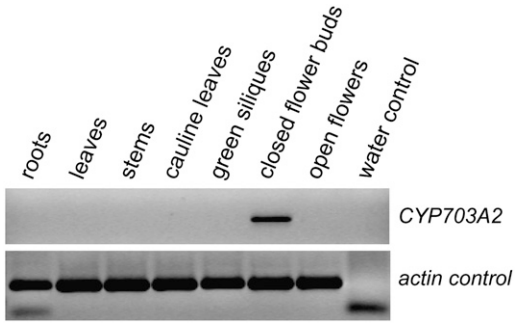

Figure 2. Detection of *CYP703A2* Transcript in Selected Tissues as Monitored by RT-PCR.

Tissues from flowering *Arabidopsis* Col-0 plants from stages 6.10 to 6.50 (Boyes et al., 2001) were analyzed for the presence of *CYP703A2* transcripts by RT-PCR. After 40 cycles of PCR, *CYP703A2* transcript was detected exclusively in closed flower buds. *Actin1* (*At2g37620*) was used as a control gene, and primers were designed to exclude the amplification of genomic DNA.

a poor pollen survival rate, and reduced filament growth. Only within the more apical flowers did the combined effects of increased filament length, slightly increased pollen viability, and increased pollen numbers serve to improve the chance of the pollen to come into direct contact with the stigma and thus enable pollination, despite impaired pollen survival and release rates (Figure 4C).

Knockout of CYP703A2 Impairs Pollen Wall Architecture

Microscopic observations of open anthers in apical flowers of the *CYP703A2* knockout lines revealed a reduction of the quantity of mature pollen, as some of the pollen grains were arrested in development. The pollen grains from anthers at the basal parts of the inflorescences were highly degenerated, and few microspores went through the entire maturation process. Accordingly, all subsequent pollen observations were based on pollen isolated from anthers from apical flowers. Mature pollen from wild-type lines as well as from the two *CYP703A2* knockout lines contained two generative cells and a single vegetative nucleus (Figures 5A to 5C), indicating that meiosis and mitosis occurred normally.

Microscopic analyses of longitudinal sections of mature anthers under UV light revealed that the characteristic fluorescent layer around the pollen grains from the *CYP703A2* knockout lines was lacking (Figures 5H and 5I). The fluorescence around the wild-type pollen originates from phenylpropanoid units that are part of the sporopollenin in the exine layer. The absence of this fluorescent layer demonstrated that the sporopollenin component of the exine layer was structurally altered or absent.

The size and shape of the microspores in the wild type and the *CYP703A2* knockout line were analyzed by scanning electron microscopy (Figure 5). Whereas wild-type microspores exhibited a uniform size, microspores from the *CYP703A2* knockout line could easily be divided into two size classes. One class contained microspores that had a similar size as wild-type spores, and the other class contained microspores that were a lot smaller (Figure 5F). At the tetrad stage, the microspore size of *CYP703A2* knockout lines was indistinguishable from that of the wild type (data not shown). This suggests that the small microspores were arrested in development after tetrad release (Figure 5F, white arrows). Analyses of mature pollen grains by scanning electron microscopy revealed that the characteristic ornamented pattern of the surface of the wild-type pollen ascribed to the exine layer was lacking in the *CYP703A2* knockout lines, which instead exhibited a smooth surface (Figures 5D to 5G). Likewise, the three characteristic furrows of the *Arabidopsis* tricolpate pollen were missing in pollen from the *CYP703A2* knockout lines. When

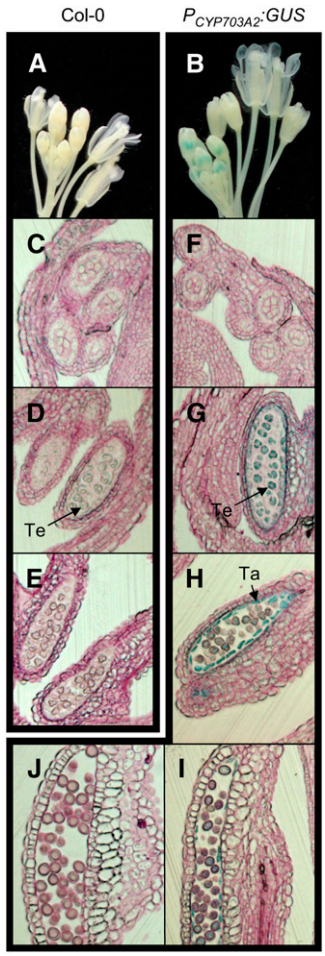

Figure 3. Floral Expression of *CYP703A2* as Analyzed by GUS Staining of Transgenic $P_{CYP703A2}$*:GUS Arabidopsis* Plants.

(A) and **(B)** Global view of GUS-stained inflorescences in wild-type **(A)** and $P_{CYP703A2}$*:GUS* **(B)** plants.
(C) to **(J)** Sections of plastic-embedded anthers after GUS staining in wild-type (**[C]** to **[E]**) and $P_{CYP703A2}$*:GUS* reporter fusion (**[F]** to **[J]**) plants.
Ta, tapetum layer; Te, tetrad.
(C) and **(F)** Meiotic stage.
(D) and **(G)** Tetrad stage.
(E) and **(H)** After tetrad release.
(I) Tapetum degeneration.
(J) After tapetum degeneration.

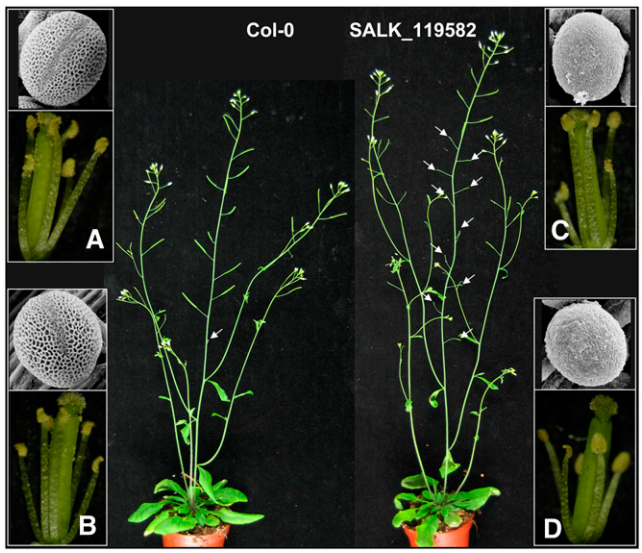

Figure 4. Comparison of Inflorescences for Col-0 and a *CYP703A2* Knockout Line.

Siliques arrested in development in the main inflorescence are indicated by white arrows. Dissection of flowers at stage 14 (Smyth et al., 1990) was done for the top part (**[A]** and **[C]**) and the middle part (**[B]** and **[D]**) of primary inflorescences. The combination of shorter filament and reduced pollen release **(D)** may explain the observed reduction of seed production for the middle part of the inflorescence. The abnormal pollen structure seen by scanning electron microscopy is conserved in the middle and top inflorescences (cf. **[A]** and **[B]** with **[C]** and **[D]**). No obvious differences were seen in the structure of pollen for the knockout between the middle and top flowers. In the *CYP703A2* knockout lines, the basal flowers displayed brown or incompletely developed anthers.

scanning electron microscopy analysis was performed without prior fixation, pollen from the *CYP703A2* knockout mutant lines collapsed, while wild-type pollen resisted the vacuum applied during fixation (cf. Figures 5D and 5F with 5E and 5G). The structural and physical protection provided by the exine layer in the wild type was thus missing in pollen from the *CYP703A2* knockout lines.

In order to analyze the structure of the mutant pollen wall in further detail, transmission electron microscopy was undertaken on mature wild-type and knockout pollen grains (Figure 6). Transmission electron microscopy sections of wild-type pollen exhibited a white layer corresponding to the intine layer that covers the plasma membrane of the pollen. The subtle dark layer covering the intine layer corresponds to nexine, the internal part of the exine layer. The external exine layer is ornamented by baculum and tectum, two types of structure that appear gray on the transmission electron microscopy sections. The invaginations within the tectum and baculum layer contain a white-gray matrix designated tryphine. Tryphine is deposited at the end of pollen development and completes the formation of the mature pollen coat. In contrast with the well-organized architecture of the wild-type pollen wall, the knockout pollen sections revealed an irregular intine layer and a total absence of the characteristic exine layer. The irregularity of the plasma membrane observed in the knockout lines might be a reflection of the lacking exine layer. In addition, small vesicles supposedly targeted with material for exine formation accumulate in the knockout lines. It is not clear whether the dark and irregular layer covering the intine corresponds to the nexine layer or a residual deposition of tryphine or a mixture of both.

CYP703 Catalyzes In-Chain Hydroxylation of Saturated Medium-Chain Fatty Acids

To characterize the catalytic function of CYP703A2, the enzyme was heterologously produced in yeast WAT11 cells optimized for the expression of plant P450s (Pompon et al., 1996). This expression system has been used as a reference system for the heterologous production of eukaryotic P450s for the past 10 years. The expression level and folding state of the P450 can be monitored by measuring the absorption of the reduced complex between P450 and carbon monoxide (Omura and Sato, 1964). The WAT11 yeast strain coexpresses the *Arabidopsis* NADPH P450 Reductase1 (ATR1), which delivers electrons from NADPH to the P450. Yeast microsomes that contained 53 pmol of CYP703A2 per milligram for microsomal protein were isolated and used in an in vitro screen for putative substrates. A range of fatty acids and phenylpropanoids were tested, as exine is thought to be composed of fatty acid–derived and phenylpropanoid-derived monomers (data not shown).

In the presence of NADPH, CYP703A2 was found to catalyze the in vitro monohydroxylation of saturated medium-chain fatty acids (C10, C12, C14, and C16), as analyzed by thin layer chromatography. Lauric acid (C12) was the preferred substrate (Figure 7). The turnover number of CYP703A2 with lauric acid as substrate (20 min^{-1}) was similar to that of CYP94A1 involved in cutin monomer synthesis (Tijet et al., 1998). Activity was not observed toward caprylic acid (saturated C8 fatty acid), stearic acid (saturated C18 fatty acid), unsaturated fatty acids like C18:1, C18:3, and C20:4, and phenylpropanoids like *trans*-cinnamic acid and *p*-coumaric acid. Microsomes isolated from untransformed WAT11 yeast cells did not catalyze the hydroxylation of fatty acids.

The substrate specificity exerted by CYP703A2 was further analyzed by gas chromatography–mass spectrometry (GC-MS). This substantiated that the C10, C12, and C14 saturated fatty acids were all monohydroxylated at carbon atom 6, 7, or 8 (Figure 7). A minute amount of hydroxylation at carbon 9 was also observed with lauric acid as substrate. Lauric acid (C12) was more efficiently hydroxylated compared to capric (C10), myristic (C14), and palmitic (C16) acids. Independent of the fatty acid chain length, carbon atom 7 was the major site of hydroxylation (Figure 7; see Supplemental Figure 2 online).

As in other eukaryotic cells, fatty acids are generally not freely available in plants but are typically bound as triglycerols or CoA esters (Browse and Somerville, 1991; Daum et al., 2007). To identify the in planta substrate and product of CYP703A2, lyophilized methanol extracts from developing wild-type flowers were incubated with yeast microsomes containing CYP703A2 and analyzed by liquid chromatography–mass spectrometry (LC-MS). As expected, free lauric acid was detected in neither the methanol extracts from the flowers nor in the microsomal

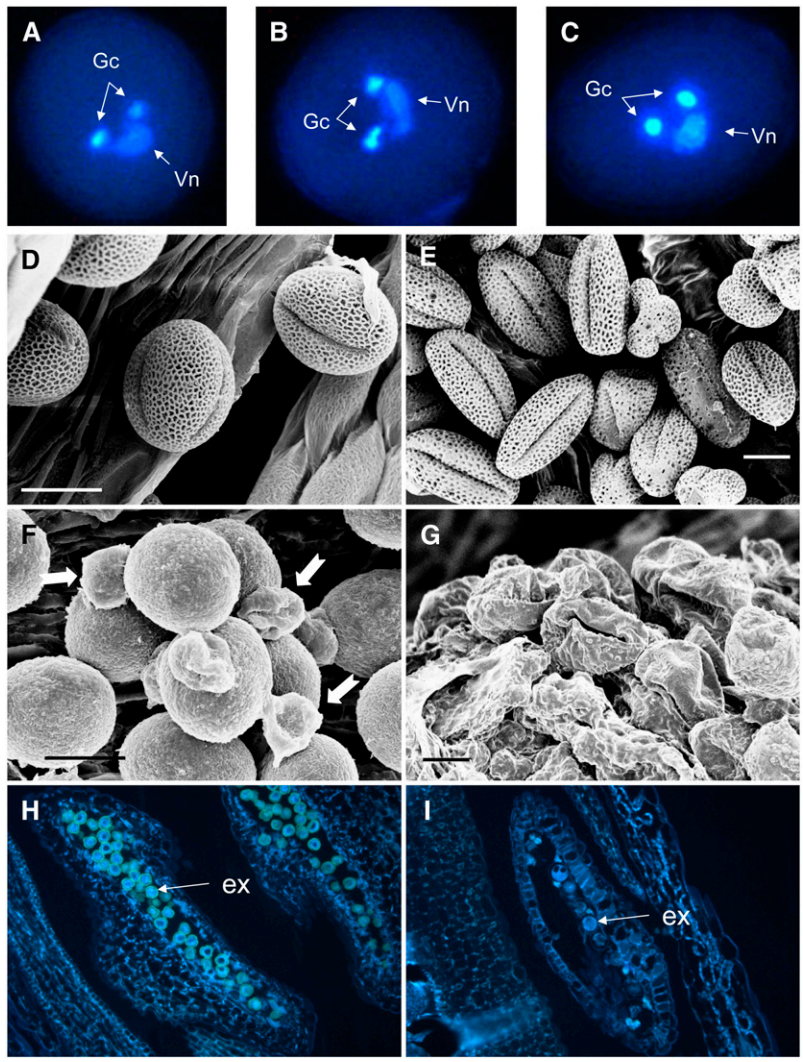

Figure 5. Comparison of Pollen from *CYP703A2* Knockout Plants and Wild-Type Pollen.

(A) to **(C)** Trinucleated *Arabidopsis* pollen in Col-0 (wild-type) **(A)**, SLAT N56842 knockout line **(B)**, and SALK_119582 knockout line **(C)**. Gc, generative cells; Vn, vegetative nucleus. Nuclei in isolated pollen from wild-type and *CYP703A2* knockout lines were visualized by staining with 4′,6-diamidino-2-phenylindole dihydrochloride.

(D) to **(G)** Surface structure of *Arabidopsis* pollen from wild-type plants (**[D]** and **[E]**) and the *CYP703A2* knockout line (**[F]** and **[G]**) after fixation of the tissues (**[D]** and **[F]**) or without fixation (**[E]** and **[G]**), monitored by scanning electron microscopy. Bars = 10 μm.

(H) and **(I)** Autofluorescence under UV irradiation of mature anthers from wild-type **(H)** and *CYP703A2* knockout **(I)** lines. Autofluorescence is impaired in the *CYP703A2* knockout line due to the lack of exine deposition. ex, site for exine deposition. The two *CYP703* knockout lines displayed identical phenotypes.

membrane preparation (data not shown). However, upon incubation of the methanolic flower extract with yeast microsomes, a large pool of free lauric acid was released, due to the activity of yeast triacylglycerol lipases and acetyl-CoA thioesterases that copurified and adhered to the microsomal membrane preparation (Figure 8A). In the presence of NADPH, lauric acid liberated from the flower extract by the yeast microsomes was metabolized by CYP703A2 into four new metabolites with a molecular mass corresponding to that of monohydroxylated lauric acid (Figure 8A, gray peaks). The same product profile was obtained when CYP703A2-containing microsomes were incubated with free lauric acid (Figure 8B). The GC-MS analyses demonstrate that the four product peaks correspond to hydroxylation at the C6, C7, C8, and C9 positions, with the main product (retention time = 21.5 min) representing hydroxylation at the C7 position. Capric acid and to some extent also myristic acid were identified as substrates in the in vitro experiments with isolated fatty acids (Figure 7). Yeast triacylglycerol lipases and acetyl-CoA thioesterases are known to exert a broad substrate specificity (Daum et al., 2007). Accordingly, release of capric or myristic acid would be expected if the corresponding conjugates were present in the flower extracts. Neither capric acid nor myristic acid or their

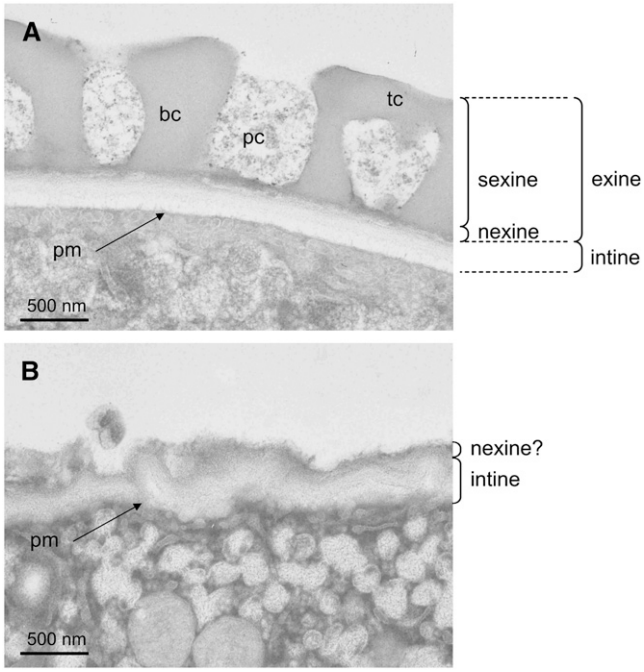

Figure 6. Ultrastructure of Pollen Wall from Wild-Type and Insertion Line SALK_119582 Plants as Seen by Transmission Electron Microscopy.

(A) Transmission electron microscopy sections of wild-type pollen coat revealed a regular intine layer covered with a nexine layer and an outer structured sexine layer with the typical ornamented structures composed of bacula and tecta and covered with pollen coat.

(B) By contrast, the exine layer was absent in both insertion lines, as seen here for the SALK line. Only an irregular intine layer is visible, together with a layer that might be the nexine layer or the residual pollen coat. Compared with the wild type, the plasma membrane of the *CYP703A2* knockout line appears highly irregular, and vesicles supposedly filled with material targeted for exine formation seem to accumulate in the cytosol.

bc, baculum; pc, pollen coat; pm, plasma membrane; tc, tectum.

corresponding monohydroxylated products could be detected when flower extracts were incubated with CYP703A2-containing yeast microsomes, which strongly indicates that lauric acid and lauric acid monohydroxylated at the C6, C7, C8, or C9 position with preferential hydroxylation at the C7 position are the in planta substrate and products of CYP703A2 (Figure 8A).

DISCUSSION

We have identified CYP703A2 as a lauric acid in-chain hydroxylase involved in exine formation. Mutants lacking CYP703A2 were male-semisterile and were characterized by a smooth pollen surface, as opposed to the usual characteristic ornamented surface (Figures 4 and 5). Several male-sterile mutants have previously been characterized with reduced or abolished exine wall. *flp1* has an altered pollen surface (Ariizumi et al., 2003). FLP1 has been suggested to play a role in the synthesis of the tryphine, the mixture of fatty acids and proteins embedded within the exine layer (Figure 6) and responsible for pollen hydration and pollen–stigma interaction and recognition. In contrast with *CYP703A2*, *FLP1* is also expressed in stems and siliques. The *nef1* mutant is also impaired in exine development. NEF1 is a chloroplastic membrane protein that may be involved in either lipid biosynthesis or lipid transport (Ariizumi et al., 2004), underpinning the importance of lipids in exine biosynthesis. The mutant *dex1*, lacking the exine characteristic pattern, has been described as defective in a membrane-associated protein (At3g09090) most likely involved in early exine (primexine) formation (Paxson-Sowders et al., 2001). Based on the phenotype, expression patterns, and catalytic function of CYP703A2, we propose to name the two *CYP703A2* knockout mutants *dex2-1* (SLAT N56842) and *dex2-2* (SALK_119582), for *defective in exine patterning2*.

In angiosperms, male sterility can occur due to dysfunctions in anther and pollen development (Sanders et al., 1999). Some mutant lines are male-sterile, while in other mutants, only a reduction of fertility is observed. Mutants affected in exine development, like *ms2*, encoding a protein homologous with fatty acid reductases (Aarts et al., 1997), often exhibit reduced seed set. Like the *CYP703A2* knockout mutant *dex2*, *MS2* is expressed during pollen maturation and *ms2* mutants have brown and shrivelled anthers, reduced production of pollen grains, and the majority of the seeds are produced from apical flowers formed at the inflorescence. Both the *ms2* mutant and the *CYP703A2* knockout mutant *dex2* characterized in this study exhibit impaired pollen walls, and the development defect is observed after the pollen mother cell has undergone meiosis (Aarts et al., 1997). The strong phenotypic resemblance between these two mutants suggests that both loci could serve key functions in sporopollenin synthesis and exine production. Based on these two mutants, we conclude that sporopollenin deposition during exine formation is important but not essential for seed production in *Arabidopsis*.

CYP703A2 Is a Lauric Acid in-Chain Hydroxylase

The impaired exine production in the *CYP703A2* knockout lines (Figures 4 to 6) and the ability of CYP703A2 to catalyze in-chain monohydroxylation of medium-chain fatty acids (Figure 7) indicate that CYP703A2 provides medium-chain hydroxy fatty acids as essential building blocks during sporopollenin synthesis and exine formation. When in-chain hydroxy lauric acids are not formed, the fluorescent layer around the pollen ascribed to sporopollenin is absent. This lack of in-chain hydroxylated lauric acids prevents the formation of cross-links in the form of ester and ether linkages between the two key building blocks of sporopollenin. Methanol extracts from developing flowers revealed the presence of a large pool of conjugated lauric acid that may serve as an intermediate storage form of lauric acid for sporopollenin biosynthesis. The absence of capric (C10) and myristic (C14) esters in flower extracts further argues that lauric acid (C12) is the in planta substrate of CYP703A2. This is in agreement with the in vitro screening that identified lauric acid as the best substrate (Figure 7). Accordingly, in-chain monohydroxylated lauric acids are essential building blocks in sporopollenin synthesis and thus are required for proper pollen

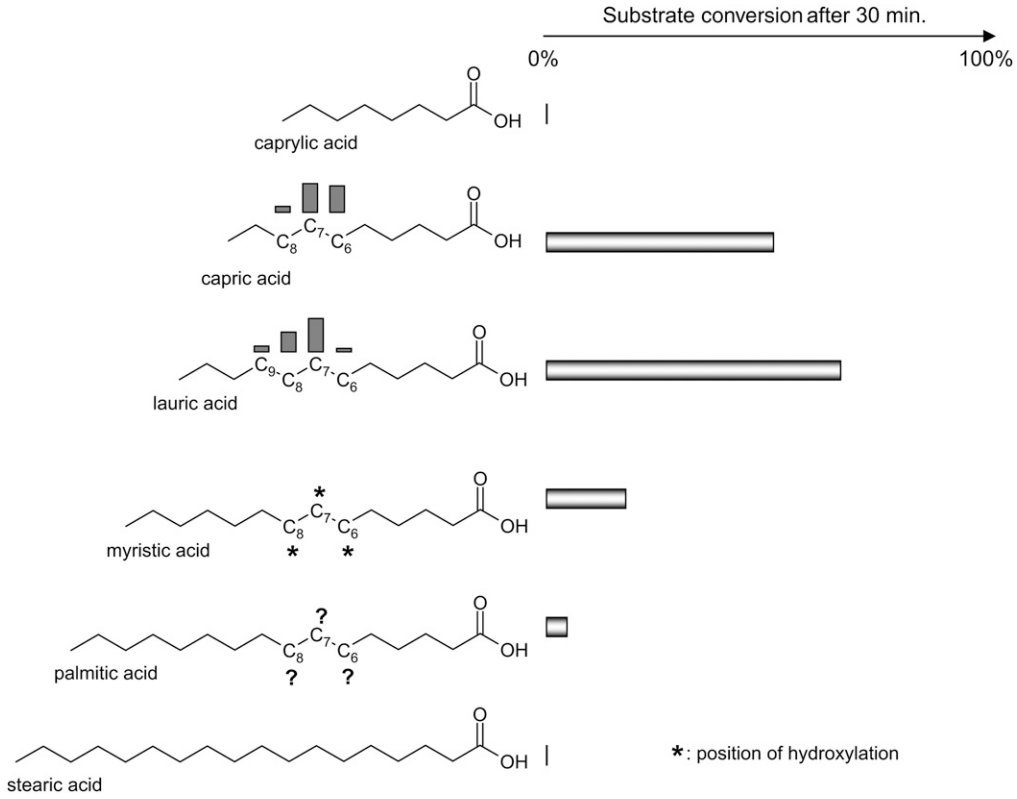

Figure 7. CYP703A2-Catalyzed Hydroxylation of Fatty Acids of Different Chain Lengths and Identification of Carbon Atom 7 as the Main Site of Hydroxylation.

Medium-chain saturated fatty acids were incubated in the presence of 10 pmol of CYP703A2, and products were analyzed by thin layer chromatography and GC-MS. For hydroxy capric acid and hydroxy lauric acid, the horizontal gray bars represent the relative ratio of hydroxylation for each carbon. Due to the low conversion rates, the relative ratios could not be determined for hydroxy myristic acid. For the same reason, the position of the hydroxylation of palmitic acid could not be determined. Three potential hydroxylation sites (?) are proposed based on the observed hydroxylation patterns for capric, lauric, and myristic acids.

development and viability. Hydroxy lauric acids possess a hydroxy as well as a carboxy group that, together with phenylpropanoid units like *p*-coumaric or caffeic acid (Wehling et al., 1989), provide oxygen atoms required for the formation of ether and ester linkages during biosynthesis of the sporopollenin polymer (Guilford et al., 1988; Ahlers et al., 2003). Ahlers et al. (2000, 2003) previously suggested the presence of aliphatic units containing more than one oxygen atom in sporopollenin of cattail. The documented ability of CYP703A2 to preferentially hydroxylate carbon atom 7 of lauric acid offers a route to synthesize building blocks that secure a uniform distance between the cross-links in sporopollenin. This provides increased resistance to evaporation by controlling the level of reticulation of the pollen wall. The presence of additional ether linkages originating from other hydroxy groups residing in phenylpropanoids would further augment the strong resistance of the polymer to chemical degradation.

Independent of fatty acid chain length, CYP703A2 preferentially catalyzed hydroxylation at carbon atom 7 (Figure 7). This catalytic property is unique for a plant fatty acid hydroxylase, as most other fatty acid hydroxylases are end chain (ω) hydroxylases (Kandel et al., 2006). Accordingly, we propose that in CYP703A2, the fatty acid carboxy group is positioned deep within the active site and anchors the fatty acid with the hydrophobic chain tightly secured in the binding pocket of the enzyme, thus facilitating in-chain hydroxylation independent of fatty acid chain length, preferentially at the C7 position (Figure 7). A similar orientation of fatty acids has been observed in CYP152A1 from *Bacillus subtilis*, which catalyzes hydroxylation at the α- or β-carbon (C2 or C3) of long-chain free fatty acids. In CYP152A1, the carboxy group interacts with the positively charged guanidinium group of Arg-242 in the I-helix and thus positions the substrate so that the α- or β-carbon is in proximity to the heme within the active site (Lee et al., 2003). By contrast, in the *Bacillus megaterium* fatty acid ω-1- or ω-2-hydroxylase ($P450_{BM-3}$ or CYP102), the fatty acid carboxy function is positioned at the entrance of the substrate access channel and thus serves to position the substrate with the ω position in proximity to the heme (Ravichandran et al., 1993). A similar orientation of the fatty acid has been suggested for CYP81B1 from *Helianthus tuberosus*, which is an ω-1- to ω-5-hydroxylase (Cabello-Hurtado et al., 1998). Future crystal structures or homology modeling studies

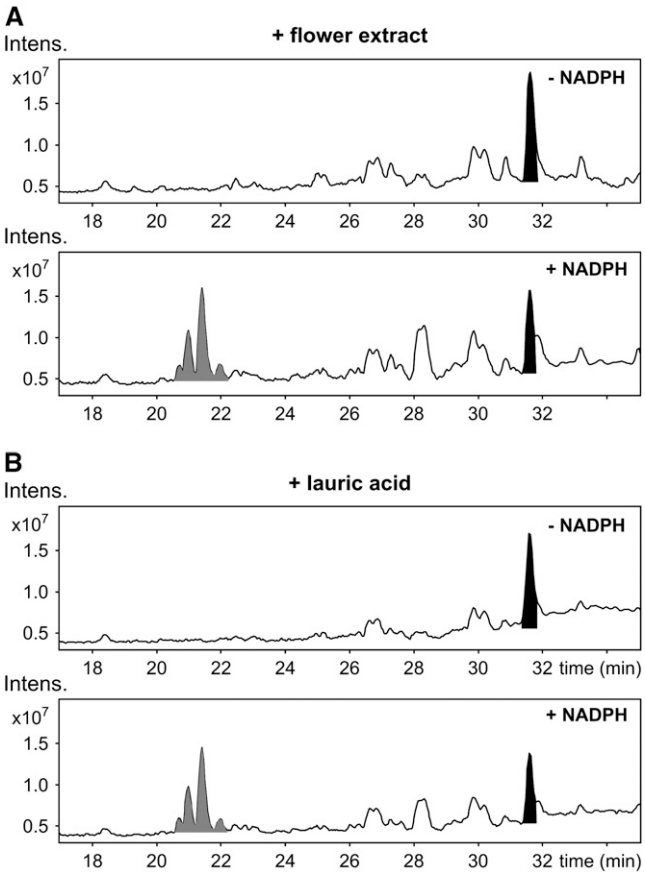

Figure 8. LC-MS Chromatograms of the Incubation of CYP703A2 with Flower Extract and Lauric Acid.

(A) Methanol extracts from wild-type *Arabidopsis* flowers were used for in vitro incubations with yeast microsomes containing CYP703A2 in the presence or absence of NADPH. In the presence of NADPH, lauric acid (black peaks) was converted into four monohydroxy lauric acid products (gray peaks), as characterized by extracted ion chromatography.
(B) The same product pattern was observed when 10 nmol of lauric acid was used as a substrate.

should help to elucidate how lauric acid is positioned in the active site of CYP703A2.

CYP703A2 Coexpresses with Genes Involved in Exine Formation

The formation of exine and the biosynthesis of the sporopollenin polymer involve multiple genes. To identify putatively coregulated genes, the Genevestigator microarray database (Zimmermann et al., 2004) was mined using *CYP703A2* as the query. Two genes previously known to be involved in pollen development after the meiotic step, *At4g14080* ($r^2 = 0.9149$) and *MS2* ($r^2 = 0.816$), were identified. *At4g14080* encodes a callase involved in degradation of the callose wall during pollen development (Hird et al., 1993), and *MS2* (*At3g11980*) encodes the fatty acid reductase that when mutated gives rise to the male-sterile *ms2* line (Aarts et al., 1997). According to the model proposed by Dong et al. (2005), degradation of the callose wall of the microspore occurs simultaneously with the biosynthesis of sporopollenin in primexine and exine. Thus, the observed coexpression pattern provides independent support for a key function of CYP703A2 in exine biosynthesis. A more general investigation of coexpression patterns using Expression Angler (Toufighi et al., 2005) identified several genes in phenylpropanoid synthesis, including *At4g34850*, *At1g02050* (both encoding a chalcone or stilbene synthase), *At1g62940* (encoding a 4-coumarate-CoA ligase), and *At1g68540* (encoding a cinnamoyl-CoA reductase–like protein). In addition, *At3g42960* (encoding an alcohol dehydrogenase), *At1g75790* (encoding a multicopper oxidase type I family protein), and *CYP704B1* (*At1g69500*), belonging to clan 86 comprising fatty acid hydroxylases, were identified as being coexpressed with *CYP703A2*. This coexpression pattern underpins the concerted synthesis of fatty acids and phenylpropanoids.

Evolution of CYP703, a Prerequisite for the Development of Terrestrial Plants

A major challenge encountered by the first land plants was to protect their spores from dehydration and damage by UV irradiation. The CYP703 family has been a key player in this process, and CYP703A2 is a documented example of a P450 shown specifically to be involved in pollen development. The high conservation in terrestrial plants, the specific expression in developing flowers, the conserved substrate specificity among petunia and *Arabidopsis*, and the observed deficiency with respect to pollen wall development in the T-DNA insertion lines strongly suggest that the CYP703 family is exclusively devoted to a key step in pollen development after the tetrad release stage. The general expression pattern in male tissues of gymnosperms and angiosperms (Table 1) documents a general function of the CYP703A family in pollen development of spermatophytes. Knockout of allene oxide synthase, *CYP74A*, has been shown to confer male-semisterility in *Arabidopsis* (Park et al., 2002). However, CYP74A is involved in biosynthesis of the phytohormone jasmonic acid, and the expression of *CYP74A* is not restricted to anther or pollen, in agreement with a more general role in signal transduction pathways (e.g., by wounding).

EST database searches identified *CYP703A* orthologs in angiosperms and gymnosperms (Table 1). When compared, the ESTs listed in Table 1 indicated the presence of a single *CYP703* transcript in *Picea*, *Secale*, *Triticum*, *Antirrhinum*, *Ipomoea*, and *Solanum*. In the fully annotated genomes of *Arabidopsis* and *O. sativa*, unique *CYP703* orthologs were also identified (Figure 1, Table 1). Similarly, in *Populus trichocarpa*, a single functional sequence, *CYP703A4*, and a pseudogene were identified. The recent genome duplication of the poplar genome (Blanc and Wolfe, 2004) might explain the presence of two alleles in this particular species, in which one of the alleles has become a pseudogene while the other paralog has retained the original function (Walsh, 1995). No orthologs have been identified in ferns. This may simply reflect the limited amount of sequence information available within this taxonomic group. In agreement with a unique function in terrestrial plants, no *CYP703* orthologs could be identified in the fully sequenced genome of the green

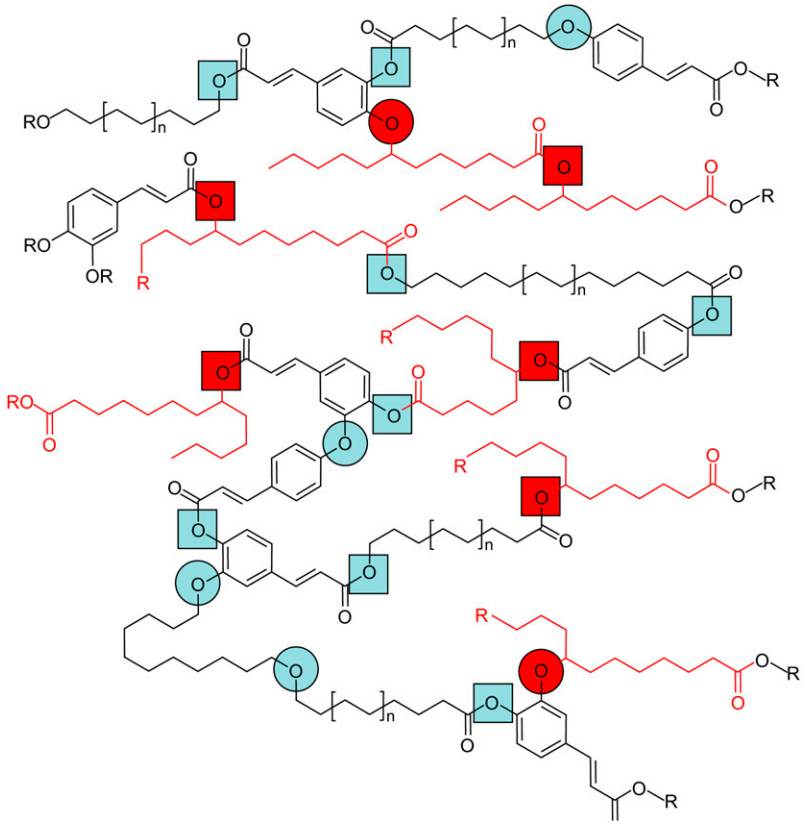

Figure 9. Model of the Role of CYP703A2 in Sporopollenin Formation.

Monomeric units derived from CYP703-catalyzed hydroxylation of lauric acids are shown in red. The participation of oxygen atoms within these units in ester and ether linkages in the formation of the sporopollenin biopolymer is illustrated by circles and squares, respectively. The *p*-coumaric and caffeic acid units illustrate the presence of phenylpropanoids in the sporopollenin polymer.

alga *C. reinhardtii* (http://www.chlamy.org/). *C. reinhardtii* constitutes a valid ancestor to land plants (Willis and McElwain, 2002), and the absence of the CYP703 family in this organism as well as other algae demonstrates that the CYP703 family appeared after the radiation of land plants from the chlorophyte group during the adaptation to a terrestrial life form.

In mosses, spores may be regarded as equivalent to pollen in that they are the result of a meiotic division and are protected by a similar cell wall composed of sporopollenin (Zetzsche et al., 1937). In agreement with this, three members of the CYP703 family, designated CYP703B1, CYP703B2, and CYP703B3, were identified in the *P. patens* genome (Figure 1, Table 1). It is not understood at present why the *P. patens* genome contains three apparently fully functional *CYP703* paralogs while the other known genomes contain a single copy. However, divergence between mosses and angiosperms occurred around 425 million years ago (Willis and McElwain, 2002), and subsequent duplication events and neofunctionalization of the *CYP703* ancestral gene could be a valid explanation. Analysis of expression patterns and heterologous expression of the enzymes encoded by the three *P. patens CYP703* paralogs should reveal whether the three gene copies are truly redundant or whether they have acquired new functions or become pseudogenes, as observed in poplar. The possibility to delete genes in *P. patens* by homologous recombination should facilitate the clarification of this issue. We suggest that at least one of the *CYP703B* alleles in *P. patens* is involved in spore wall development.

The need to protect the gametophyte is not restricted to terrestrial plants. In the salt water alga *Chlamydomonas monoica* (Chlorophyta), the zygospore is protected by the biopolymer algaenan. The algaenan biopolymer is known to contain C22, C24, and C26 fatty acids and alcohol units linked by ether and ester linkages (Blokker et al., 1999). In contrast with algaenan, sporopollenin contains phenylpropanoids that provide the necessary additional protection from UV irradiation and dehydration (Figure 5). Based on the ability of CYP703A2 to provide preferentially C7 monohydroxylated lauric acid and on the model for algaenan (Blokker et al., 1999), we propose a model for the impact of CYP703A2 in sporopollenin biosynthesis (Figure 9). Monomeric hydroxylated fatty acid units produced by CYP703 and phenylpropanoids like *p*-coumaric acid and caffeic acid joined by ether and ester linkages provide the backbone of the sporopollenin. To provide further strength to the sporopollenin polymer, additional ether linkages can be envisioned added by subsequent but currently unknown hydroxylases. Whether some of the coexpressed genes identified by Genevestigator or

Expression Angler encode hydroxylases providing additional hydroxy groups remains an open question.

The freshwater algae charophytes represent some of the most primitive organisms hosting the phenylpropanoid pathway (Kroken et al., 1996). Identification of *CYP703* orthologs in freshwater algae may provide new knowledge on the origin of sporopollenin. The occurrence of phenylpropanoid units in freshwater algae also supports the notion that the early phenylpropanoid pathway evolved before the lignin pathway. Accordingly, the lignin pathway may have evolved from the sporopollenin pathway. Thus, it is tempting to speculate that the major determinant in the evolution of the phenylpropanoid pathway was to provide monomeric aromatic units that, upon incorporation into sporopollenin freshwater algae spores, provided the necessary resistance to UV irradiation (e.g., when ponds dried out during the climatic changes that preceded the evolution of terrestrial plants).

METHODS

CYP703A Expression

Sequence Database Mining

Searches for putative *CYP703A2* orthologs were performed using TBLASTN searches (Altschul et al., 1990) (blosum62 matrix) in the plant EST database at http://www.ncbi.nlm.nih.gov/ using *Arabidopsis thaliana* CYP703A2 as the query sequence. Candidate gene sequences were analyzed for similarities to the CYP703 family by an additional BLAST (BLASTX) search in the plant P450 database at http://www.p450.kvl.dk/blast.html, currently encompassing 573 P450 sequences, including all *Arabidopsis* P450 sequences. Multiple sequence alignments and a bootstrapped neighbor-joining phylogenic tree based on 1000 iterations were constructed using ClustalX (Thompson et al., 1997) using the default parameters (Gonnet protein weight matrix series) (Gonnet et al., 1992) and MEGA 3.1 (Kumar et al., 2004), respectively, and subsequently used to confirm the assignment to the CYP703 family. The multiple sequence alignment used to construct the phylogenetic trees can be downloaded from our website (http://www.p450.kvl.dk/Figure1_Alignment_Marc.pdf).

The Gene Atlas tool at Genevestigator (https://www.genevestigator.ethz.ch/) was used to determine the expression pattern of *CYP703A2* (*At1g01280*) in *Arabidopsis*. The search included data from experiments performed with wild-type plants and the 22K *Arabidopsis* data set. At the time of the analysis, 1388 array experiments representing 1388 RNA extractions from callus (6 slides), cell suspensions (71 slides), seedlings (308 slides), inflorescences (170 slides), rosettes (626 slides), and roots (207 slides) were included in the 22K data set.

Phylogenetic Analysis

The bootstrapped neighbor-joining tree was built in MEGA 3.1 (Kumar et al., 2004) with a set of protein sequences representative of the P450s from clan 71. The two non-clan 71 P450s, CYP51A1 and CYP710A1, were used as an outgroup to root the tree, as they are ancient P450s involved in essential steps in the biosynthesis of sterols present in all plants and thus precede the occurrence of the 71 clan. The tree was bootstrapped with 1000 iterations (node cutoff value of 50%). The underlying amino acid sequences in FASTA format (see Supplemental Data 1 online) and the multiple alignment (see Supplemental Data 2 online) can be accessed at http://www.p450.kvl.dk/Review2006/Figure1_Sequence_FASTA.tfa and http://www.p450.kvl.dk/Figure1_Alignment_Marc.pdf, respectively.

CYP703A2-Promoter GUS Fusion and Plant Transformations

The 1000 nucleotides upstream of the start codon of *CYP703A2* were amplified from Col-0 genomic DNA using the primers 5′-ATACATGTAAAGCTTACGAAAGAGAAGCTGATATCGGCCTTGTCTAGAGA-3′ and 5′-CGAATATGAGGATCCCTAATCTTATATTCTATATTCAACAAGTCTTTTGA-3′ containing the restriction sites *Hin*dIII and *Bam*HI (underlined), respectively. The PCR products obtained were ligated into the binary vector pBI121 (Clontech). *Agrobacterium tumefaciens* strain LBA4404 holding the plasmid Ti pAL4404 was transformed with this construct harboring the *NPTII* gene conferring kanamycin resistance (Hoekema et al., 1983). The *Arabidopsis* lines Wassilewskija and Col-gl1 were transformed by the floral dip method (Clough and Bent, 1998). Transformed plants were selected on Murashige and Skoog agar plates supplemented with kanamycin (50 mg/L).

RNA Extractions and RT-PCR

Total RNA was extracted with the RNeasy Plant Mini kit (Qiagen) from flowers at stages 6.10 to 6.50 (Boyes et al., 2001). RNA (1 μg) was reverse-transcribed with the iScript cDNA synthesis kit (Bio-Rad), and *CYP703A2* expression was subsequently visualized by PCR with the primers 5′-TTAAAGCTCTAATTCAGGACATGATAG-3′ and 5′-CCATAAACTTCCACCGTATCAATATTTC-3′ using the Phusion High-Fidelity DNA polymerase (Finnzymes) and following the manufacturer's protocol. Forty amplification cycles were performed: 10 s at 98°C, 30 s at 60°C, and 15 s at 72°C. *Actin1* (*At2g37620*) was used as a control with the primers 5′-GGTCGTACTACCGGTATTGTGCT-3′ and 5′-TGACAATTTCACGCTCTGCT-3′. For both *CYP703A2* and *Actin1*, primers were designed to be mRNA-specific by spanning an intron.

Characterization of CYP703A2 Knockout Lines

Two T-DNA insertion lines for *At1g01280* in ecotype Col-0, SLAT N56842 and SALK_119582 (alias N619582), were obtained from the Nottingham Arabidopsis Stock Centre. Genotyping of the lines with respect to the *At1g01280* locus was done with the primers 703for2 (5′-TACCTAGGAGATTACTTGCCATTTTGGAG-3′) and 703rev2 (5′-ACGTCTCTCGTACCACACAACGTAGATAG-3′). In the SLAT N56842 line, the presence of the T-DNA insertion was detected with the primers 703for2 and dspm1 (5′-CTTATTTCAGTAAGAGTGTGGGGTTTTGG-3′) or 703rev2 and dspm11 (5′-GGTGCAGCAAAACCCACACTTTTACTTC-3′). In the SALK_119582 line, T-DNA insertion in the *At1g01280* locus was detected by PCR with the primers 703rev2 and LBa1 (5′-TGGTTCACGTAGTGGGCCATCG-3′) or 703for2 and 5′-ACTCTAATTGGATACCGAGGGGAATTTAT-3′. PCR fragments containing T-DNA border sequences were sequenced for verification of the T-DNA insertion (see Supplemental Figure 1 online).

Histology

Petals and sepals of *Arabidopsis* flowers were removed by dissection using a Leica MZ FLIII stereomicroscope fitted with a Leica DC 300F camera. Anther sections were analyzed using a Leica DMR fluorescence microscope, likewise fitted with a Leica DC 300F camera.

Arabidopsis flowers were embedded in plastic according to the manufacturer's manual for Technovit 8100 (Heraeus) with minor alterations. The tissues were dehydrated in a graded series of acetone solutions (25, 50, and 100%, 1 h each) and left overnight in the filtration solution. Sections (5 μm) were cut on a Reichert-Jung 2030 rotary microtome. Mature anthers were dissected and pollen grains released in a solution of mannitol (0.3 M) and 4′,6-diamidino-2-phenylindole dihydrochloride (0.3 μM) (Fluka). After incubation, pollen grains were analyzed with a Leica DMR fluorescence microscope.

GUS colorations were performed on freshly harvested plants by a swift ethanol (70%) wash followed by incubation (37°C, 16 h) in GUS staining

solution (Jefferson, 1989). Stained tissues were dehydrated by successive washes in ethanol solutions of increasing strength (50 to 96%). GUS sections were counterstained with periodic acid Schiff, starting with an overnight incubation in dimedon (0.5%). The following day, sections were washed in running tap water (15 min) followed by incubation (10 min) in freshly made periodic acid (1%). Before incubation in Schiff reagent (30 min), the sections were washed (running tap water, 10 min). Directly from the Schiff reagent, the sections were incubated (3 × 2 min) in $Na_2S_2O_5$ (0.5%). Finally, the sections were rinsed (running tap water, 10 min), followed by a brief wash (1 min) in ion-exchanged water.

For scanning electron microscopy, dissected flowers were vacuum-infiltrated with a solution of glutaraldehyde (2.5%) and paraformaldehyde (2%) in phosphate buffer (0.1 M, pH 7.2). Flowers were washed three times with a phosphate buffer (0.1 M, pH 7.2), dehydrated in a graded series of ethanol, critical-point dried (CPD 020; Balzers Union), and mounted on specimen stubs using double-sided tape. The samples were coated with gold:palladium (3:2) in an ion sputter (JFC-1100; JEOL) and analyzed with a scanning electron microscope (LEO 435VP) with secondary electron detector at high voltage (10 kV). Plants analyzed without prior fixation were infiltrated with phosphate buffer (0.1 M, pH 7.2).

For transmission electron microscopy analysis, the anthers were vacuum-infiltrated and fixed with 2.5% glutaraldehyde and 2% paraformaldehyde in 100 mM Na-phosphate buffer, pH 7.0, for 3 h. Samples were postfixed in 1% osmium tetroxide for 2 h, dehydrated in acid dimethoxypropane and acetone, and embedded in Spurr resin (Ted Pella). Ultrathin sections were stained with uranyl acetate and lead citrate and observed with a JEM-1010 transmission electron microscope (JEOL).

Heterologous Expression in Yeast

The *CYP703A2* cDNA was amplified by PCR from the flower cDNA library CD4-6 (Weigel et al., 1992) using the primers 5′-CGATATTCTTGGATCC-ATGATTTTGGTGCTAGCCTCC-3′ and 5′-CGATATTCTTGGTACCTTA-TGTGTACAAATGAGCTGC-3′ harboring the restriction sites *Bam*HI and *Kpn*I (underlined) and ligated into pGEM-T (Promega). The internal *Bam*HI site in *CYP703A2* was removed by quick-change strategy mutagenesis (Stratagene). The verified coding sequence was inserted in the multicopy shuttle vector pYeDP60 and subsequently transformed into *Saccharomyces cerevisiae* strain WAT11, engineered to coexpress ATR1 (Pompon et al., 1996). Expression of CYP703A2 was induced by galactose (Pompon et al., 1996), and expression levels were estimated by carbon monoxide difference spectrometry (Omura and Sato, 1964).

In Vitro Enzyme Assays with Lipid Substrates and Flower Extracts

Microsomes (10 mg protein/mL, 10 pmol of P450) isolated from yeast expressing CYP703A2 were incubated (30 min) with a series of radiolabeled fatty acids (100 μM) of different chain lengths in Na-phosphate buffer (50 mM, pH 7.4). After incubation, the reaction mixture was applied to a thin layer chromatography plate (Silica Gel 60 F_{254} sheets; Merck) and developed in diethyl ether:light petroleum:formic acid (50:50:1, v/v/v) (Pinot et al., 1998). For GC-MS analysis, products were eluted from the thin layer chromatography plates with diethyl ether:hexane (50:50, v/v; 10 mL), methylated with diazomethane, and silylated with a mixture of pyridine and *N*,*O*-bistrimethylsilyltrifluoroacetamide containing 1% (v/v) trimethylchlorosilane (1:1, v/v). GC-MS analysis was performed using an Agilent 6890 series gas chromatograph fitted with a capillary column (0.25 mm × 30 m, 0.25-μm film thickness [HP-5MS]). The gas chromatograph was combined with a quadrupole mass selective detector (Agilent 5973N). Mass spectra were recorded (70 eV) and analyzed as described by Eglinton et al. (1968).

Flowers from inflorescences containing flowers at every stage of development, from small buds to the last stage before silique elongation, were extracted with hot methanol. Floral tissues (500 mg) were boiled for 5 min in 1 mL of 85% methanol. Twenty microliters of this extract were lyophilized and subsequently used as substrate for in vitro assays with CYP703A2, as described above. Control assays were performed with 100 μM lauric acid. After 30 min of incubation at 28°C, reaction mixtures were stopped by the addition of ethyl acetate, concentrated in vacuum, and analyzed by LC-MS.

LC-MS was performed using a HP1100 liquid chromatograph (Agilent Technologies) coupled to a Bruker Esquire 3000+ ion trap mass spectrometer (Bruker Daltonics). An XTerra MS C18 column (Waters; 3.5 μm, 2.1 × 100 mm) was used at a flow rate of 0.2 mL/min. The mobile phases were A (0.1% [v/v] HCOOH and 50 μM NaCl) and B (0.1% [v/v] HCOOH and 80% [v/v] MeCN). The gradient program was as follows: 0 to 2 min, isocratic 18% B; 2 to 30 min, linear gradient 18 to 100% B; 30 to 50 min, isocratic 100% B. The spectrometer was run in negative electrospray mode.

Plant Culture Conditions

Plants were cultivated in an autoclaved mixture of soil:vermiculite (medium size) (2:1, v/v) and grown in insect-free climate chambers with 16 h of light (100 μE intensity) at 21°C and 75% humidity.

Accession Numbers

Accession number for ESTs can be found in Table 1; amino acid sequences in FASTA format used for the construction of the phylogenetic tree can be found as Supplemental Data 1 online and at http://www.p450.kvl.dk/Review2006/Figure1_Sequence_FASTA.tfa.

Supplemental Data

The following materials are available in the online version of this article.

Supplemental Figure 1. Positions of T-DNA Insertions in *dex2-1* and *dex2-2*.

Supplemental Figure 2. GC-MS Analyses of Metabolites Produced by CYP703A2 on Capric, Lauric, and Myristic Acids.

Supplemental Data 1. FASTA File of Amino Acid Sequences Used for the Construction of the Phylogenetic Tree.

Supplemental Data 2. Multiple Sequence Alignment Used for the Construction of the Phylogenetic Tree.

ACKNOWLEDGMENTS

We thank Jonathan Jones at the Sainsbury Laboratory (John Innes Center, Norwich UK) for providing the SLAT T-DNA insertion line, Joseph R. Ecker and the Salk Institute Genomic Analysis Laboratory for providing the sequence-indexed T-DNA insertion mutant, and the ABRC for distributing the seeds. We also thank Kerstin Brismar and Salla Martina for assistance in scanning electron microscopy; Carl Erik Olsen for LC-MS analyses; Christina Lunde for helpful discussions on *P. Patens*; Suzanne M. Paquette for help with bioinformatics and for data mining the poplar genome for *CYP703* orthologs; and finally Julia Hosp, Ron Coolbaugh, and Peter Hedden for valuable scientific discussions.

Received July 15, 2006; revised April 1, 2007; accepted April 18, 2007; published May 11, 2007.

REFERENCES

Aarts, M.G.M., Hodge, R., Kalantidis, K., Florack, D., Wilson, Z.A., Mulligan, B.J., Stiekema, W.J., Scott, R., and Pereira, A.

(1997). The *Arabidopsis* MALE STERILITY 2 protein shares similarity with reductases in elongation/condensation complexes. Plant J. **12:** 615–623.

Ahlers, F., Bubert, H., Steuernagel, S., and Wiermann, R. (2000). The nature of oxygen in sporopollenin from the pollen of *Typha angustifolia* L. Z. Naturforsch. [C] **55:** 129–136.

Ahlers, F., Lambert, J., and Wiermann, R. (2003). Acetylation and silylation of piperidine solubilized sporopollenin from pollen of *Typha angustifolia* L. Z. Naturforsch. [C] **58:** 807–811.

Ahlers, F., Thom, I., Lambert, J., Kuckuk, R., and Rolf, W. (1999). ^{1}H NMR analysis of sporopollenin from *Typha angustifolia*. Phytochemistry **50:** 1095–1098.

Alonso, J.M., et al. (2003). Genome-wide insertional mutagenesis of *Arabidopsis thaliana*. Science **301:** 653–657.

Altschul, S.F., Gish, W., Miller, W., Meyers, E.W., and Lipman, D.J. (1990). Basic local alignment search tool. J. Mol. Biol. **215:** 403–410.

Ariizumi, T., Hatakeyama, K., Hinata, K., Inatsugi, R., Nishida, I., Sato, S., Kato, T., Tabata, S., and Toriyama, K. (2004). Disruption of the novel plant protein NEF1 affects lipid accumulation in the plastids of the tapetum and exine formation of pollen, resulting in male sterility in *Arabidopsis thaliana*. Plant J. **39:** 170–181.

Ariizumi, T., Hatakeyama, K., Hinata, K., Sato, S., Kato, T., Tabata, S., and Toriyama, K. (2003). A novel male-sterile mutant of *Arabidopsis thaliana*, faceless pollen-1, produces pollen with a smooth surface and an acetolysis-sensitive exine. Plant Mol. Biol. **53:** 107–116.

Bedinger, P. (1992). The remarkable biology of pollen. Plant Cell **4:** 879–887.

Blanc, G., and Wolfe, K.H. (2004). Widespread paleopolyploidy in model plant species inferred from age distributions of duplicate genes. Plant Cell **16:** 1667–1678.

Blokker, P., Schouten, S., de Leeuw, J.W., Sinninghe Damsté, J.S., and van den Ende, H. (1999). Molecular structure of the resistant biopolymer in zygospore cell walls of *Chlamydomonas monoica*. Planta **207:** 539–543.

Bohne, G., Richter, E., Woehlecke, H., and Ehwald, R. (2003). Diffusion barriers of tripartite sporopollenin microcapsules prepared from pine pollen. Ann. Bot. (Lond.) **92:** 289–297.

Boyes, D.C., Zayed, A.M., Ascenzi, R., McCaskill, A.J., Hoffman, N.E., Davis, K.R., and Gorlach, J. (2001). Growth stage-based phenotypic analysis of *Arabidopsis*: A model for high throughput functional genomics in plants. Plant Cell **13:** 1499–1510.

Browse, J., and Somerville, C. (1991). Glycerolipid synthesis: Biochemistry and regulation. Annu. Rev. Plant Physiol. Plant Mol. Biol. **42:** 467–506.

Bubert, H., Lambert, J., Steuernagel, S., Ahlers, F., and Wiermann, R. (2002). Continuous decomposition of sporopollenin from pollen of *Typha angustifolia* L. by acidic methanolysis. Z. Naturforsch. [C] **57c:** 1035–1041.

Cabello-Hurtado, F., Batard, Y., Salaün, J.-P., Durst, F., Pinot, F., and Werck-Reichhart, D. (1998). Cloning, expression in yeast, and functional characterization of CYP81B1, a plant cytochrome P450 that catalyzes in-chain hydroxylation of fatty acids. J. Biol. Chem. **273:** 7260–7267.

Clough, S.J., and Bent, A.F. (1998). Floral dip: A simplified method for *Agrobacterium*-mediated transformation of *Arabidopsis thaliana*. Plant J. **16:** 735–743.

Daum, G., Wagner, A., Czabana, T., and Athenstaedt, K. (2007). Dynamics of neutral lipid storage and mobilization in yeast. Biochimie **89:** 243–248.

Dong, X., Hong, Z., Sivaramakrishnan, M., Mahfouz, M., and Verma, D.P. (2005). Callose synthase (CalS5) is required for exine formation during microgametogenesis and for pollen viability in *Arabidopsis*. Plant J. **42:** 315–328.

Edlund, A.F., Swanson, R., and Preuss, D. (2004). Pollen and stigma structure and function: The role of diversity in pollination. Plant Cell **16 (suppl.):** S84–S97.

Eglinton, G., Hunneman, D.H., and McCormick, A. (1968). Gas chromatographic-mass spectrometric studies of long chain hydroxy acids. Org. Mass Spectrom. **1:** 593–611.

Galbraith, D.W., and Bak, S. (2005). Functional genomics of the cytochrome P450 gene superfamily in *Arabidopsis thaliana*. In Plant Functional Genomics, D. Leister, ed (Binghamton, NY: Haworth Press), pp. 595–620.

Gonnet, G.H., Cohen, M.A., and Brenner, S.A. (1992). Exhaustive matching of the entire protein sequence database. Science **257:** 1609–1610.

Guilford, W.J., Schneider, D.M., Labovitz, J., and Opella, S.J. (1988). High resolution solid state ^{13}C NMR spectroscopy of sporopollenins from different plant taxa. Plant Physiol. **86:** 134–136.

Hird, D.L., Worrall, D., Hodge, R., Smartt, S., Paul, W., and Scott, R. (1993). The anther-specific protein encoded by the *Brassica napus* and *Arabidopsis thaliana* A6 gene displays similarity to beta-1,3-glucanases. Plant J. **4:** 1023–1033.

Hoekema, A., Hirsch, P.R., Hooykaas, P.J.J., and Schilperoort, R.A. (1983). A binary plant vector strategy based on separation of vir- and T-region of the *Agrobacterium tumefaciens* Ti-plasmid. Nature **303:** 179–180.

Imaishi, H., Matsumoto, Y., Ishitobi, U., and Ohkawa, H. (1999). Encoding of a cytochrome P450-dependent lauric acid monooxygenase by CYP703A1 specifically expressed in the floral buds of *Petunia hybrida*. Biosci. Biotechnol. Biochem. **63:** 2082–2090.

Jefferson, R.A. (1989). The GUS reporter gene system. Nature **342:** 837–838.

Kandel, S., Sauveplane, V., Orly, A., Diss, L., Benveniste, I., and Pinot, F. (2006). Cytochrome P450-dependent fatty acid hydroxylases in plants. Phytochem. Rev. **5:** 359–372.

Kroken, S.B., Graham, L.E., and Cook, M.E. (1996). Occurrence and evolutionary significance of resistant cell walls in charophytes and bryophytes. Am. J. Bot. **83:** 1241–1254.

Kumar, S., Tamura, K., and Nei, M. (2004). MEGA3: Integrated software for molecular evolutionary genetics analysis and sequence alignment. Brief. Bioinform. **5:** 150–163.

Lee, D.-S., Yamada, A., Sugimoto, H., Matsunaga, I., Ogura, H., Ichihara, K., Adachi, S.-i., Park, S.-Y., and Shiro, Y. (2003). Substrate recognition and molecular mechanism of fatty acid hydroxylation by cytochrome P450 from *Bacillus subtilis*. J. Biol. Chem. **278:** 9761–9767.

Morant, M., Bak, S., Moller, B.L., and Werck-Reichhart, D. (2003). Plant cytochromes P450: Tools for pharmacology, plant protection and phytoremediation. Curr. Opin. Biotechnol. **14:** 151–162.

Nelson, D.R., Schuler, M.A., Paquette, S., Werck-Reichhart, D., and Bak, S. (2004). Comparative genomics of *Oryza sativa* and *Arabidopsis thaliana*. Analysis of 727 cytochrome P450 genes and pseudogenes from a monocot and a dicot. Plant Physiol. **135:** 756–772.

Ohnishi, T., Watanabe, B., Sakata, K., and Mizutani, M. (2006). CYP724B2 and CYP90B3 function in the early C-22 hydroxylation steps of brassinosteroid biosynthetic pathway in tomato. Biosci. Biotechnol. Biochem. **70:** 2071–2080.

Omura, T., and Sato, R. (1964). The carbon monoxide-binding pigment of liver microsomes. II. Solubilization, purification, and properties. J. Biol. Chem. **239:** 2379–2385.

Park, J.H., Halitschke, R., Kim, H.B., Baldwin, I.T., Feldmann, K.A., and Feyereisen, R. (2002). A knock-out mutation in allene oxide synthase results in male sterility and defective wound signal transduction in *Arabidopsis* due to a block in jasmonic acid biosynthesis. Plant J. **31:** 1–12.

Paxson-Sowders, D.M., Dodrill, C.H., Owen, H.A., and Makaroff, C.A. (2001). DEX1, a novel plant protein, is required for exine pattern

formation during pollen development in Arabidopsis. Plant Physiol. **127:** 1739–1749.

Pinot, F., Benveniste, I., Salaun, J.P., and Durst, F. (1998). Methyl jasmonate induces lauric acid omega-hydroxylase activity and accumulation of CYP94A1 transcripts but does not affect epoxide hydrolase activities in *Vicia sativa* seedlings. Plant Physiol. **118:** 1481–1486.

Pompon, D., Louerat, B., Bronine, A., and Urban, P. (1996). Yeast expression of animal and plant P450s in optimized redox environments. Methods Enzymol. **272:** 51–64.

Ravichandran, K.G., Boddupalli, S.S., Hasemann, C.A., Peterson, J.A., and Deisenhofer, J. (1993). Crystal structure of hemoprotein domain of P450BM-3, a prototype for microsomal P450's. Science **261:** 731–736.

Sanders, P.M., Bui, A.Q., Weterings, K., McIntire, K.N., HsuPei, Y.C., Lee, Y., Truong, M.T., Beals, T.P., and Goldberg, R.B. (1999). Anther developmental defects in *Arabidopsis thaliana* male-sterile mutants. Sex. Plant Reprod. **11:** 297–322.

Smyth, D.R., Bowman, J.L., and Meyerowitz, E.M. (1990). Early flower development in *Arabidopsis*. Plant Cell **2:** 755–767.

Thompson, J.D., Gibson, T.J., Plewniak, F., Jeanmougin, F., and Higgins, D.G. (1997). The ClustalX windows interface: Flexible strategies for multiple sequence alignment aided by quality analysis tools. Nucleic Acids Res. **25:** 4876–4882.

Tijet, N., Helvig, C., Pinot, F., Le Bouquin, R., Lesot, A., Durst, F., Salaün, J.P., and Benveniste, I. (1998). Functional expression in yeast and characterization of a clofibrate-inducible plant cytochrome P-450 (CYP94A1) involved in cutin monomer synthesis. Biochem. J. **332:** 583–589.

Toufighi, K., Brady, S.M., Austin, R., Ly, E., and Provart, N.J. (2005). The Botany Array Resource: E-northerns, expression angling, and promoter analyses. Plant J. **43:** 153–163.

Walsh, J.B. (1995). How often do duplicated genes evolve new functions? Genetics **139:** 421–428.

Wehling, K., Niester, C., Boon, J.J., Willemse, M.T.M., and Wiermann, R. (1989). *p*-Coumaric acid—A monomer in the sporopollenin skeleton. Planta **179:** 376–380.

Weigel, D., Alvarez, J., Smyth, D.R., Yanofsky, M.F., and Meyerowitz, E.M. (1992). LEAFY controls floral meristem identity in *Arabidopsis*. Cell **69:** 843–859.

Werck-Reichhart, D., Bak, S., and Paquette, S. (April 14, 2002). Cytochromes P450. In The Arabidopsis Book, C.R. Somerville and E.M. Meyerowitz, eds (Rockville, MD: American Society of Plant Biologists), doi/10.1199/tab.0009, http://www.aspb.org/publications/arabidopsis/.

Willis, H.J., and McElwain, J.C. (2002). The Evolution of Plants. (Oxford, UK: Oxford University Press), pp. 156–193.

Zetzsche, F., Kalt, P., Liechti, J., and Ziegler, E. (1937). Zür Konstitution des Lycopodium-Sporonins, des Tasmanins und des Lange-Sporonins. XI. Mitteilung über die Membran der Sporen und Pollen. J. Praktische Chemie **148:** 267–286.

Zimmermann, P., Hirsch-Hoffmann, M., Hennig, L., and Gruissem, W. (2004). GENEVESTIGATOR. Arabidopsis microarray database and analysis toolbox. Plant Physiol. **136:** 2621–2632.